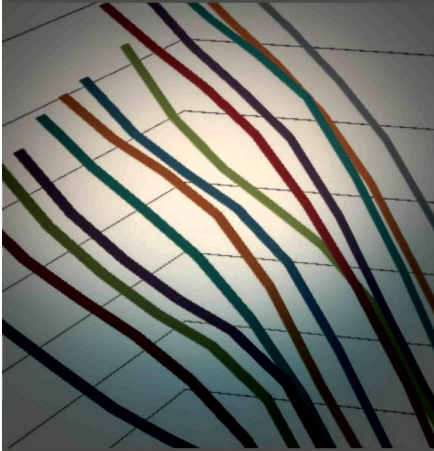


Lacunarity of the Spatial Distributions of Soil Types in Europe

J. Caniego Monreal*
F. San José Martínez
J.J. Ibáñez Martí
R. Pérez-Gómez



Lacunarity as a means of quantifying textural properties of spatial distributions suggests a classification into three main classes of the most abundant soils that cover 92% of Europe. Soils with a well-defined self-similar structure of the linear class are related to widespread spatial patterns that are non-dominant but ubiquitous at continental scale.

Fractal techniques have been increasingly and successfully applied to identify and describe spatial patterns in natural sciences. However, objects with the same fractal dimension can show very different optical properties because of their spatial arrangement. This work focuses primary attention on the geometrical structure of the geographical patterns of soils in Europe. We made use of the European Soil Database to estimate lacunarity indexes of the most abundant soils that cover 92% of the surface of Europe and investigated textural properties of their spatial distribution. We observed three main classes corresponding to three different patterns that displayed the graphs of lacunarity functions, that is, linear, convex, and mixed. They correspond respectively to homogeneous or self-similar, heterogeneous or clustered and those in which behavior can change at different ranges of scales. Finally, we discuss the pedological implications of that classification.

Abbreviations: RA, regionally abundant pedotaxa; RS, regionally sparse pedotaxa; WA, widespread abundant pedotaxa; WS, widespread spread pedotaxa.

It is well-known that spatial distributions of soil surface systems follow complex patterns and often exhibit scale-dependent changes in structure (Phillips, 2001a, 2001b). Initially, geostatistics was applied for spatial analysis mainly of single soil properties (McBratney et al., 2000), excluding soil types or pedotaxa. Later mathematical tools of biodiversity (Magurran, 1988) were applied to pedological entities (Ibáñez et al., 1990, 1994, 1995). Thus began a new branch of pedometrics called pedodiversity analysis (McBratney et al., 2000).

Fractal analysis was soon a topic of interest among pedologists (Burrough, 1981). However, as in the case of geostatistics, these mathematical tools were mainly applied to the study of single soil properties and mainly focused on soil physics and hydrology (e.g., Armstrong, 1986; Tyler and Wheatcraft, 1989), with some exceptions involving soil survey activities (Arnold 1990). A compendium on the application of fractals in soil sciences was prepared by Pachepsky et al. (2000).

In the last decades, pedodiversity analysis and fractal geometry have been used to analyze spatial distribution patterns (Ibáñez et al., 1990, 1995, 2005a, 2005b, 2009; Phillips, 2001a, 2001b). Power law relationships, a common feature of geometrical fractals, were reported for the rank-abundance lists (Zipf's law), the distribution of the areal extend of pedotaxa (Pareto distribution), and pedorichness–area curves, over more than three orders of magnitude. Caniego et al. (2006, 2007), considering pedotaxa-abundance distributions as probability measures or mass distributions, showed that pedodiversity distributions at the planetary scale of continental and island landmasses followed well-defined multifractal patterns and analyzed the use of the generalized Rényi dimensions as pedodiversity indicators (San José Martínez and Caniego, 2013).

This work focuses primary attention on the fractal structure of the geographical patterns of soil spatial distributions in Europe. As fractal objects with the same fractal dimension can show very different geometrical and textural properties (Mandelbrot, 1983) because of their spatial arrangement, it appears that new fractal parameters need to be added to characterize fractal geometrical structures. In a coarse sense, fractal dimension accounts for the regularity trend across scales of the way fractal objects occupy the space and that information should be completed with other fractal parameters that describe the morphology of their geometric configuration (Allain and Cloitre, 1991).

Lacunarity was introduced by Mandelbrot (1983) to quantify textural properties of spatial distribution of data sets. In the last decade, lacunarity has been applied to describe spatial patterns in earth science, environmental sciences, and ecology. Plotnick et al. (1993, 1996) made use of lacunarity functions as indicators of landscape texture and as a general technique to describe patterns of spatial dispersion. Myint and Lam (2005) observed that lacunarity approaches can be used to improve digitally classifying urban land-use and land-cover classes. Hoechstetter et al. (2011) adopted lacunarity analysis to compare three-dimensional surface patterns in terms of their degree of heterogeneity in landscape ecology. Also, soil fractal structure (Turcotte, 1997) has been characterized by lacunarity indexes (Zeng et al., 1996, Kim et al., 2007, Chung et al., 2008; Luo and Lin, 2009). These applications involve the analysis of digital images mostly obtained from tomography imaging or provided by GIS systems. Pendleton et al. (2005) explore some implications of the use of image analysis to estimate lacunarity and Dong (2000, 2009) offers valuable information when working in a GIS environment.

We applied the concept of lacunarity to investigate the behavior of the spatial distribution of pedotaxa in Europe. We made use of the European Soil Database to classify the most abundant pedotaxa that cover 92% of the surface of Europe. Lacunarity were estimated with the algorithm of Allain and Cloitre (1991). Lacunarity graphs of these pedotaxa displayed three different patterns, that is, linear, convex, and mixed. They correspond respectively to homogeneous or self-similar, heterogeneous or clustered, and those which behavior can change at different ranges of scales. Finally, pedological interpretation of that classification will be discussed.

Theory

Lacunarity provides a method to analyze, describe, and characterize spatial patterns. It is based on the study of translational invariance of the probability distribution of the amount of sites occupied by the solid two-dimensional shape of interest along a certain domain in a range of scales. The most used method to estimate lacunarity was developed by Allain and Cloitre (1991). A box of side length r is placed at the origin of the digital map (i.e., square with M by M pixels) on the upper left corner. The number of occupied sites within the box (box mass equal to s) were determined, indicating the number of pixels, s , $0 \leq s \leq r^2$ where the considered pedotaxa is present. The box is moved one pixel along the map, and the box mass is again counted. This process was repeated to cover the pixels of the entire digital map, then producing a frequency distribution of the number of boxes of size r and mass s , $n(s, r)$. This frequency distribution is converted into a probability distribution $Q(s, r)$ when dividing by the total number of boxes $N(r)$ of size r . The first and second moment, $Z(1) = \sum s Q(s, r)$ and $Z(2) = \sum s^2 Q(s, r)$, of this probability distribution were determined. The lacunarity for this box size r is defined as

$$L(r) = \frac{Z(2)}{Z(1)^2}$$

A simple substitution of the moments in terms of mean μ and variance σ^2 of the distribution gives the more understandable expression

$$L(r) = \frac{\sigma^2}{\mu^2} + 1$$

It allowed us to identify lacunarity with the variance to mean ratio and to understand the concept through the measure of the dispersion of the corresponding probability distribution. This calculation is repeated over a range of box sizes, $r = 2^k$ for $k = 1, 2, 3, \dots$ and log-log plot of the lacunarity $L(r)$ versus the size r of the gliding box is then produced.

The shape of the resulting graphs may be related to several morphological features of the spatial distribution of soil types. For each value of the box size r , $L(r)$ depends on the areal extent of the set being smaller for greater extensions. The range of the lacunarity log-log graphs goes from zero for the greater scale to the logarithm of the inverse of the occupancy ratio for unit boxes, that is., the logarithm of the inverse of the areal fraction of the set of interest. Lacunarity values also depend on the box sizes decreasing with increasing sizes because larger boxes are more invariant by translations. Then, log-log lacunarity graphs decrease from their maximum, which is attained at the smallest considered box, to zero, which corresponds to the greatest considered box.

The rate of change of the log-log representation of the lacunarity function is an indicator of the textural properties along the range of scales that have being considered (Plotnick et al., 1993; Dong, 2000). A fast decreasing rate of lacunarity functions corresponds to random or homogeneous structures that usually display concave up shapes. The extreme case of this type of behavior corresponds to a regular set with equidistant points, and it gives a straight line with slope tending to be vertical. A slower rate decrease of lacunarity appears for clustered structures that show concave down shapes. This type of log-log lacunarity graph usually falls rapidly to zero for a certain scale. This scale indicates typical cluster size. Between these two cases, log-log lacunarity can present slight concavity with little variations of the rate of change. A particularly interesting case of this behavior corresponds to graphs close to a straight line. They correspond to self-similar sets with fractal dimension related to the slope. This property can be used to determine the degree of self-similarity and to estimate the fractal dimension.

Table 1. List of the 45 more abundant pedotaxa with abbreviation of the soil classification of the World Reference Base of FAO, areal extent, and geographical attribute.

Pedotaxa	Abbreviation	Attribute†	Area	Pedotaxa	Abbreviation	Attribute†	Area
			km ²				km ²
Haplic Podzols	PZha	RS	1,618,480	Histic Albeluvisols	ABhi	RA	449,485
Distric Cambisols	CMdy	WA	1,475,636	Calcic Chernozems	CHcc	WS	447,101
Eutric Cambisols	CMeu	WA	1,421,705	Albic Phaeozems	PHab	RA	421,772
Distric Regosols	RGdy	RA	11,14,164	Calcaric Regosols	RGca	WS	407,032
Distric Histosols	HSdy	RA	1,091,501	Eutric Regosols	RGeu	WS	357,706
Haplic Luvisols	LVha	WA	1,083,882	Distric Gleysols	GLdy	WS	347,633
Umbric Albeluvisols	ABum	RS	975,487	Chromic Cambisols	CMcr	RA	339,547
Haplic Arenosols	ARha	WA	833,050	Fibric Histosols	HSfi	WS	339,195
Distric Leptosols	LPdy	WA	801,744	Entic Podzols	PZet	WS	331,464
Haplic Leptosols	LPha	RA	798,268	Endeutric Albeluvisols	ABeu	WS	311,982
Gleyic Luvisols	LVgl	RA	746,024	Stagnic Albeluvisols	ABst	RS	307,163
Rendzic Leptosols	LPrz	RS	711,172	Leptic Podzols	PZle	WS	305,968
Gleyic Podzols	PZgl	RA	670,389	Luvic Chernozems	CHlv	RS	300,741
Chromic Luvisols	LVcr	RA	634,253	Calcaric Leptosols	LPca	WS	299,828
Rock Outcrops	Rocks	RS	603,334	Rustic Podzols	PZrs	WS	290,996
Gleyic Albeluvisols	ABgl	RS	597,353	Gleyic Cambisols	CMgl	WS	275,878
Calcaric Cambisols	CMca	RS	584,636	Luvic Phaeozems	PHlv	WS	268,776
Gelic Histosols	HSge	RA	535,008	Calcaric Fluvisols	FLca	WS	252,847
Humic Gleysols	GLhu	RS	530,313	Eutric Leptosols	LPeu	RA	250,762
Eutric Fluvisols	FLeu	RS	528,092	Distric Fluvisols	FLdy	WS	246,658
Eutric Histosols	HSeu	WS	483,597	Haplic Phaeozems	PHha	WS	219,660
Chernic Chernozems	CHch	RS	459,309	Mollic Cambisols	CMmo	RA	196,403
Eutric Gleysols	GLeu	WS	453,690				

† WA, widespread abundant pedotaxa; WS, widespread sparse pedotaxa; RA, regionally abundant pedotaxa; RS, regionally sparse pedotaxa.

Materials and Methods

To investigate the spatial heterogeneity of the soil surface system, we considered the spatial distribution patterns of the most abundant pedotaxa in Europe (45 soil types that cover 92% of Europe) of the European Soil Database (V2.0) (European Commission, 2004). We used the soil classification of the World Reference Base (1999 version) (FAO, 1999) at the second level. Table 1 displays the list of the 45 pedotaxa considered in this study with their abbreviations and area in square kilometers. Pedotaxa abbreviations correspond to those in the World Reference Base. Figure 1 shows the rank-abundance list of the pedotaxa that conforms to a power law function. Pedotaxa were ordered by geographical extent of each particular soil.

We conducted lacunarity analysis for spatial heterogeneity measurement in a GIS environment. Of the three main types of GIS data—raster, vector, and tin—the raster data structure provides the richest modeling environment and operators for spatial analysis. The GIS raster technology provides a large number of geoprocessing and analytical tools: distance and density functions,

interpolation and surface analysis methods, and statistical functions. When working with geographic data, we often have the entire population to work with, so descriptive statistics rather than inferential statistics are used.

We used the ESRI program ArcGIS® Spatial Analyst to implement the gliding box method developed by Allain and Cloitre (1991). This program provides a set of statistical functions, which makes descriptive statistics part of our geographic analysis. The statistical functions in a raster GIS are basically classified into local or cell statistics, neighborhood or focal statistics, and zonal statistics. While local statistic functions allow processing many raster data sets together, neighborhood statistic functions can discover trends within a single raster data set based on the values within a specified group of cells, which surround and usually include the evaluation cell. This technique, that is similar to the use of a filter over the data set, is the method we applied in this work.

We considered a study area of 6000 by 6000 km covering the whole Europe. By doing so, we could get an exact number of rows and columns in all the raster data sets obtained in the vector to raster

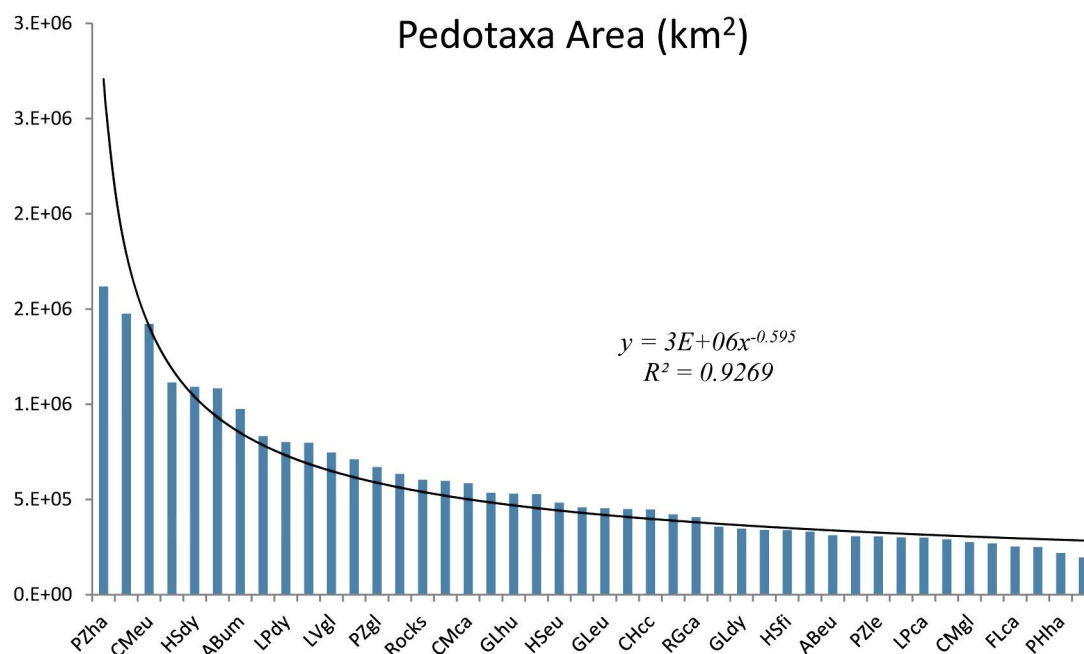


Fig. 1. Rank/abundance plot of total area occupied by each of the pedotaxa, ranked by size of the 45 most abundant pedotaxa in Europe. It follows a power law function where very few pedotaxa cover large areas, and most of them cover very small ones.

processes of the vector soil polygons. This helped us to prevent from artifacts in the “cell values” and, in turn, in the analysis results. We applied the neighborhood statistics methods to any of the soil type data set in raster format to implement the gliding box method. These raster data sets have an initial resolution of 10 km, that is, 1 cm at scale 1:1,000,000. We computed the number of cells, within the moving box, where the geographical feature was present (1 = presence, 0 = absence). This number is called mass of the box. The output raster layer with mass values was obtained when moving the box from left to right and from top to bottom. Then, lacunarity values were computed with the statistical values of this output raster data set.

To avoid inconsistencies in the results, some preprocessing such as masking and reclassification were required before applying the algorithm. The process is repeated with different window size $r = 2^k$ for $k = 1, \dots, 8$ to get the different points of the lacunarity graphs. These curves represent log–log relationships, where the x axis corresponds to the logarithm of the size of the moving box and the y axis to the logarithm of the lacunarity value.

Results and Discussion

Figure 2 shows graphs of the lacunarity functions of Haplic Podzol soil obtained with minimum box sizes equal to 10, 20, and 40 km. These graphs illustrate the typical behavior of analyzed soils, and they are consistent with numerical experiments of Plotnick et al. (1993, 1996). The intermediate minimum size 20 km was selected to analyze patterns of pedotaxa spatial distribution. This choice

improved the reliability of the analysis as the size of the smallest polygon of the digital soil map of Europe is 5 km. Therefore, the European map was covered with 90,000 unit boxes of 20-km side length each. The greatest box contains 256^2 unit boxes. It represents a square of 5120-km side length that is very close to the total map size. We expressed the size of the gliding box as the number r of unit boxes that cover its side length. We considered values $r = 2^k$ where $k = 1, \dots, 8$ as it is common in the literature. The lacunarity functions $L(r)$ are represented in log–log plots.

The initial value of the log–log lacunarity graphs (see Fig. 2 for the particular case of Haplic Podzol soil) corresponded to unit box and it was related to the extension of pedotaxa. As stated above, it was equal to log of the inverse value of the fraction of occupied cells by the pedotaxa, that is, its fraction areal extent. The last value, which corresponds to the greatest scale, is equal to zero. Therefore, to discriminate different properties through the analysis of lacunarity graphs, soil types should have similar extensions.

Inspection of lacunarity log–log plots shows three different patterns: concave, linear, and a mixture of both. Concave down shape may be associated to clustered or concentrate pedotaxa. The graph decreases slowly at small scales because lacunarity values tend to stabilize. This indicates a high dispersion of the mass box distribution, that is, very different box masses. If pedotaxa appears located at compact areas in a dense manner, the boxes occupancy rate takes a wide range of values. But, the graph decays at a certain intermediate scale. That scale can be used to find the minimum size of clusters of pedotaxa space distribution. Linear shape of the

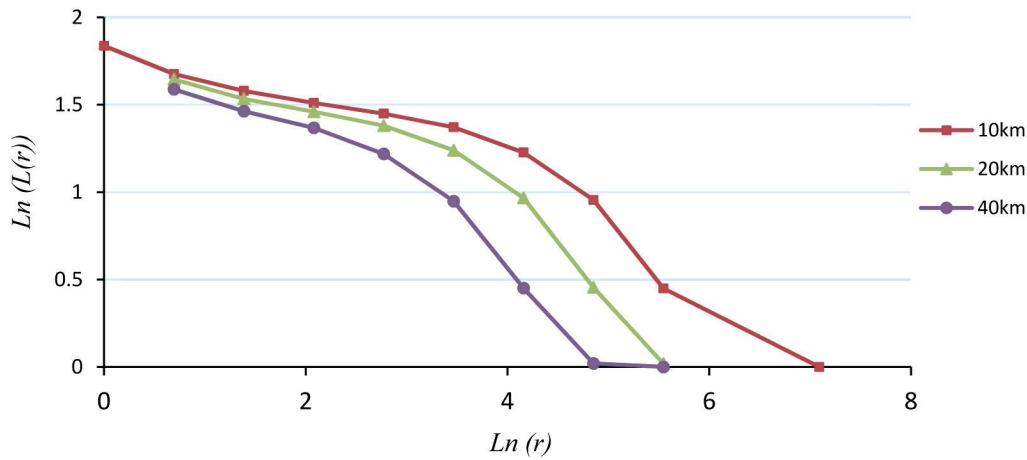


Fig. 2. Graphs of the lacunarity function for minimum box sizes 10, 20, and 40 kms for the most abundance pedotaxa Haplic Podzol (PZha). These graphs are consistent with numerical experiments.

lacunarity functions is a sign of invariance of the textural clustering behavior of the pedotaxa distributions respect to scale. It indicates a constant decrease of lacunarity for increasing scales, that is, it changes at the same speed with the scale. This pattern corresponds to homogeneously distributed pedotaxa. This property is related to the degree of self-similarity of a given structure and is independent of its areal extent. Self-similar sets present scale invariance in a visual inspection, and their lacunarity graphs are straight lines whose slope depends on its fractal dimension (Allain and Cloitre, 1991). Also, this linear pattern can describe random or uniform structures as particular cases of self-similarity. The third pattern can produce changes on concavity. The change from linear shape to concave shape indicates that clustered texture is detected. Finally, let us note that we did not find any pedotaxa in Europe in which the log–log lacunarity graph displays a concave up shape. This type of concavity corresponds to the spatial homogeneity of unstructured random processes as white noise (Plotnick et al., 1993). Soil forming factors confer spatial structure to the soil spatial distributions that should preclude the occurrence of this type of concave up lacunarity graphs.

To establish quantitative boundaries to distinguish between geographical distributions patterns, the deviation of log–log lacunarity graphs from the linear behavior would be considered. Therefore, we made use of the coefficient of determination of the linear fit R^2 to discriminate between those patterns. The values of 0.94 and 0.98 were selected as the limits to define these three groups because they provide a rough classification of the log–log lacunarity plots into three visually similar classes. Pedotaxa with coefficient of variation smaller than 0.94 would be classified as concave, pedotaxa with R^2 values greater than 0.98 would be classified as linear, and pedotaxa with coefficients between 0.94 and 0.98 would belong to the mixed type.

Figure 3 shows lacunarity graphs of the concave group. An example of this behavior is shown in Fig. 6a. This map displays the distribution of RGdy pedotaxa (in red) where solid regions with predominantly uniform red-colored areas are interwoven with green porous regions corresponding to other soils. Figure 4 shows lacunarity plots of the linear type corresponding to linear log–log lacunarity graphs. In this case, the texture of the spatial distribution of pedotaxa shows disaggregated red patches and dense green regions corresponding to other pedotaxa. Figure 6b illustrates this behavior where CMdy pedotaxa (in red) form the porous area of the green region where other pedotaxa are located. Let us note that this behavior can be observed at every scale, and they have a self-similar structure as they have a linear log–log lacunarity graph and therefore a well-defined fractal dimension. Figure 5 corresponds to the mixed group with light or changing concavity graphs. Figure 6c displays the spatial distribution of LVha pedotaxa where an intermediate behavior is apparent.

Figure 7 shows the relationship of pedotaxa ordered by areal extent (on the vertical axis) with the coefficient of determination (on the horizontal axis) of the corresponding log–log lacunarity graph. Vertical lines correspond to the values of R^2 that delimitate the three different patterns, that is, concave, mixed, and linear, from left to right. Let us note that all pedotaxa with concave graphs have large areal extent. The linear group contains more pedotaxa, but also this is the group with more variety when the areal extent is considered. The mixed group has an intermediate behavior. This group does not have as many soils as the linear group but contains a great variety of sizes as compared with the concave group.

In Europe some soil types are ubiquitous, while other ones are confined to specific geographical areas. However, this does not mean that all of the most ubiquitous pedotaxa are necessarily very abundant. There are soil types with a small area but that are widespread across the continent, and there are others of great areal extent that

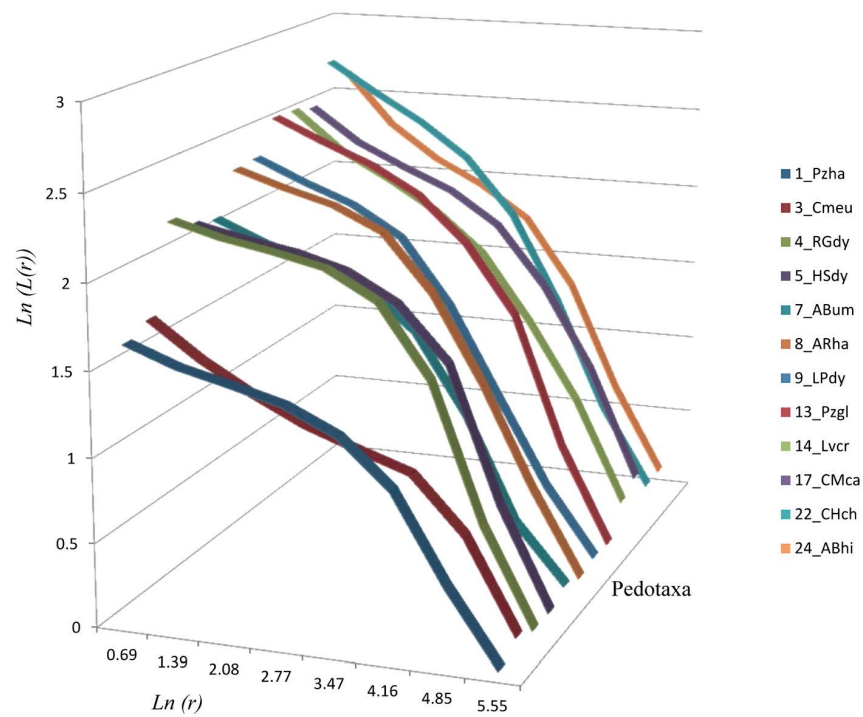


Fig. 3. Lacunarity graphs for pedotaxa (ordered areal extent_abbreviation) of the concave group.

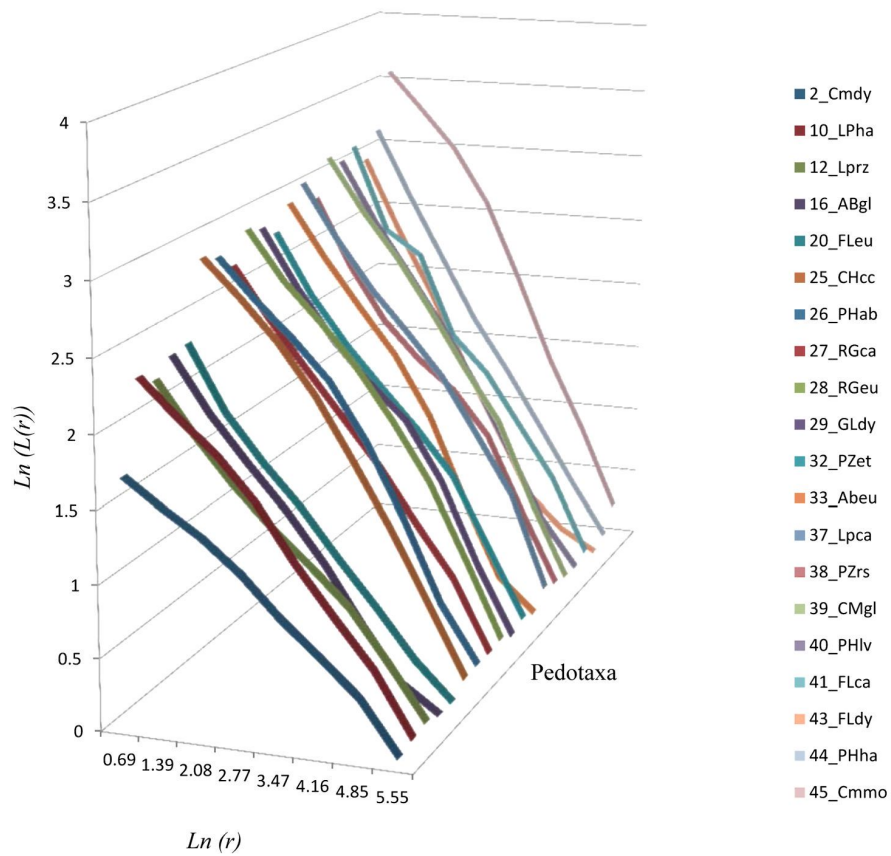


Fig. 4. Lacunarity graphs for pedotaxa (ordered areal extent_abbreviation) of the linear group.

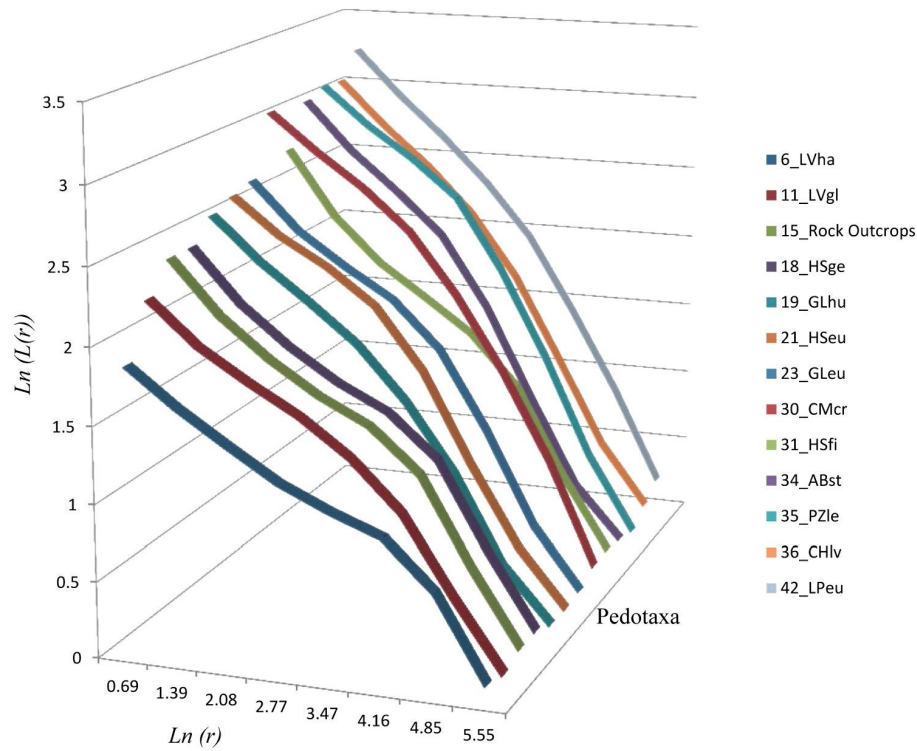


Fig. 5. Lacunarity graphs for pedotaxa (ordered areal extent_abbreviation) of the mixed type group.

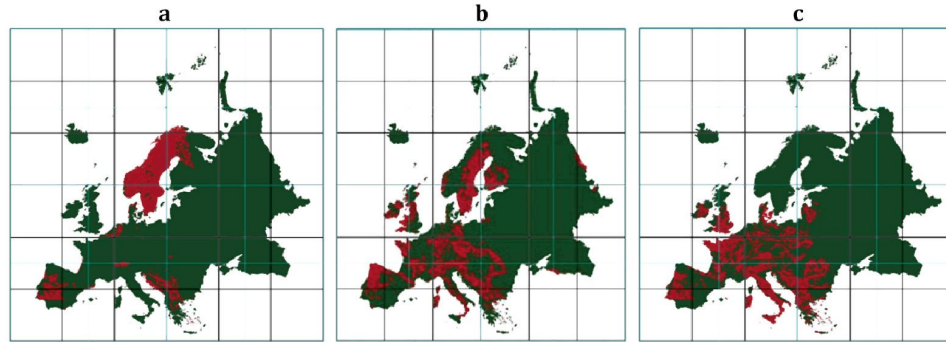


Fig. 6. Europeans maps and lacunarity graphs of the pedotaxa representing different lacunarity behavior. (a) Concave: Distric Regosols (RGdy) is a regionally abundant pedotaxa (RA) (b) Linear: Distric Cambisols (CMdy) is a widespread and abundant pedotaxa (WA) with a well-defined self-similar structure. (c) Mixed type: Haplic Luvisols (LVha) is a widespread and abundant pedotaxa (WA) that has a lacunarity graph that changes from linear to concave behavior and as a consequence does not display a well-defined self-similar structure.

are confined to a particular region in Europe. Therefore, we can differentiate between ubiquitous and regional soil types. Furthermore, some abundant soil types are also widespread at a continental level or strongly biased to certain geographical regions. Obviously, the degree of ubiquity and geographical dispersion varies according to the pedotaxa studied and thus a geographical characterization of the pedotaxa emerges according to the following occurrence categories (see Table 1): (i) widespread and abundant pedotaxa (WA), that is, dominant and ubiquitous soils at continental scale; (ii) regionally abundant

pedotaxa (RA), that is, regional dominant soils; (iii) nonabundant and sparse but widespread pedotaxa (WS), that is, nondominant and ubiquitous soils at continental scale; (iv) nonabundant, sparse, and regionally distributed pedotaxa (RS), that is, nonabundant regional subordinate soils; and (v) rare soils, that is, endemic soils. Notice that the last category refers to those pedotaxa that cover very small areas and are probably restricted to certain geographical sites. Because of the fact that we only investigated the most abundant pedotaxa, none of the soil classes considered in this study contains endemic soils.

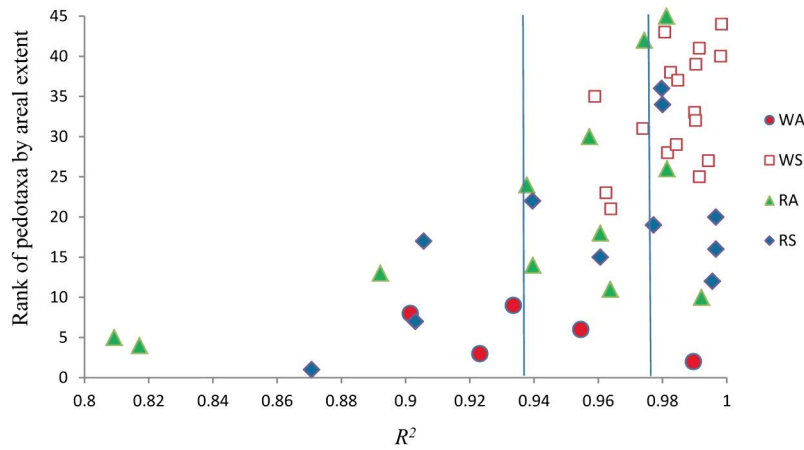


Fig. 7. Relationship between pedotaxa ordered by area and coefficient of determination with geographical attributes: widespread abundant pedotaxa (WA), widespread sparse pedotaxa (WS), regionally abundant pedotaxa (RA), and regionally sparse pedotaxa (RS).

The previous geographical characterization is compared with our lacunarity analysis in Fig. 7. This graph suggests that each geographical type has a tendency to dominate on a particular area of the region embraced by the axes of Fig. 7. This fact might suggest the geographical meaning of the lacunarity classification in three categories of soils across Europe. Geographical type WS dominates the upper linear region that corresponds to self-similar structures with small areal extent. Type WA is located in the lower part of the graph corresponding to big pedotaxa in terms of areal extent. They mostly belong to concave lacunarity group. RS soils have an intermediate areal extent and belong to any lacunarity type, while RA soils generally fit on the concave and mixed lacunarity regions of the graph and may have any areal extent. Therefore, geographical attributes seems to indicate that the self-similar structures of the linear group are related to widespread soils that are nondominant and ubiquitous at continental scale. These soils are small continental structures when considering their areal extent with a well-defined self-similar behavior. Dominant and ubiquitous soils at continental scale are big continental structures that generally do not have a well-defined self-similar structure. Also, regional soils of any kind have a tendency to display non-self-similar features, but they may have any areal extent.

This study seems to indicate that there should be a certain relationship between pedotaxa size and well-defined self-similar behavior. Our results suggest that the size of the scenario (Europe) and the chosen resolution (20 km) allow perceiving the self-similar features of pedotaxa with small areal extent. Then, we got an upper and a lower cut-off to explore the structure of the spatial distribution of self-similar pedotaxa. In terms of extension, most soils with intermediate and big size do not display well-developed self-similar structures. Therefore, lacunarity could account for the adequate size of the scenario and the right resolution to study self-similar features. Let us note that self-similar patterns have linear log–log lacunarity plots in which slope is related to their fractal dimension.

So, lacunarity do not provide new information when self-similar structures are the object of interest. Nevertheless, lacunarity could be a kind of self-similarity test. As a consequence, other fractal parameters, like local porosity or configurational entropy (Andraud et al., 1997), should be explored to determine their ability as qualitative descriptors of textural features of the fractal structure of pedotaxa distributions.

Conclusions

To investigate the spatial heterogeneity of the soil surface system, we considered the spatial distribution patterns of the most abundant 45 soil types in Europe that cover 92% of the total extension. Lacunarity analyses have been conducted with the gliding box method to investigate the geographical distribution of European soil types.

Our results suggest that the different types of log–log lacunarity graphs induce a classification of pedotaxa in Europe into linear, convex, and mixed types. They correspond, respectively, to homogeneous or self-similar, heterogeneous or clustered, and those with light concavity that changes with scale. Geographical attributes seems to indicate that the self-similar structures of the linear group are related to widespread soils that are nondominant and ubiquitous soils at continental scale. Dominant ubiquitous soils at continental scale are big continental structures that generally do not have a well-defined self-similar structure. Also, regional soils of any kind have a tendency to display non-self-similar features, but they may have any areal extent.

These findings seem to indicate that lacunarity is a better descriptor of textural properties of landscapes than fractal dimension. Fractals parameters as lacunarity provide a promising mathematical tool to develop a quantitative characterization of geographical distribution of pedotaxa.

Acknowledgments

This work has been partially supported by the Plan Nacional de Investigación Científica, Desarrollo e Innovación Tecnológica (I+D+i) under Reference AGL2011-25175, Spain, and UPM (Technical University of Madrid), Reference Q060245024.

References

- Allain, C., and M. Cloitre. 1991. Characterizing the lacunarity of random and deterministic fractal sets. *Phys. Rev. A* 44(6):3552–3558. doi:10.1103/PhysRevA.44.3552
- Andraud, C., A. Beghdadi, E. Haslund, R. Hilfer, J. Lafait, and B. Virgin. 1997. Local entropy characterization of correlated random microstructures. *Physica A* 235:307–318. doi:10.1016/S0378-4371(96)00354-8
- Armstrong, A.C. 1986. On a fractal dimension of some transient soil properties. *J. Soil Sci.* 37:641–652. doi:10.1111/j.1365-2389.1986.tb00393.x
- Arnold, R.W. 1990. Fractal dimensions of some soil map units. In: *Transactions 14th International Congress of Soil Science, Kyoto, Japan*. Vol. 5. 12–18 August 1990. International Society of Soil Science, Kyoto, Japan. p. 92–97.
- Burrough, P.A. 1981. Fractal dimension of landscapes and other environmental data. *Nature* 294:240–242. doi:10.1038/294240a0
- Caniego, J., J.J. Ibáñez, and F. San José Martínez. 2006. Selfsimilarity of pedotaxa distributions at planetary level: A multifractal approach. *Geoderma* 134:306–317. doi:10.1016/j.geoderma.2006.03.007
- Caniego, F.J., J.J. Ibáñez, and F. San José Martínez. 2007. Rényi dimensions and pedodiversity indices of the earth pedotaxa distribution. *Nonlinear Processes Geophys.* 14:547–555. doi:10.5194/npg-14-547-2007
- Chung, H.Ch., D. Giménez, and S.W. Yoon. 2008. Morphology, lacunarity and entropy of intra-aggregate pores: Aggregate size and soil management effects. *Geoderma* 146:83–93. doi:10.1016/j.geoderma.2008.05.018
- Dong, P. 2000. Test of a new lacunarity estimation method for image texture analysis. *Int. J. Remote Sens.* 21:3369–3373. doi:10.1080/014311600750019985
- Dong, P. 2009. Lacunarity analysis of raster datasets and 1D, 2D and 3D point patterns. *Comput. Geosci.* 35:2100–2110. doi:10.1016/j.cageo.2009.04.001
- European Commission. 2004. *The European Soil database. Version 2.0. [CD-ROM]* EU-ESBN, IES, JRC, Brussels, Belgium.
- FAO. 1999. *World reference base for soil resources*. World Soil Resources Rep. 84. ISSS–ISRIC–FAO, Rome.
- Hoehstetter, S., U. Walz, and N.X. Thinh. 2011. Adapting lacunarity techniques for gradient-based analyses of landscape surfaces. *Ecol. Complex.* 8:229–238. doi:10.1016/j.ecocom.2011.01.001
- Ibáñez, J.J., J. Caniego, F. San-José, and C. Carrera. 2005a. Pedodiversity-area relationships for islands. *Ecol. Modell.* 182:257–269. doi:10.1016/j.ecolmodel.2004.04.005
- Ibáñez, J.J., J. Caniego, and A. García Álvarez. 2005b. Nested subset analysis and taxa-range size distributions of pedological assemblages: Implications for biodiversity studies. *Ecol. Modell.* 182:239–256. doi:10.1016/j.ecolmodel.2004.04.004
- Ibáñez, J.J., S. De-Alba, F.F. Bermúdez, and A. García-Álvarez. 1995. Pedodiversity: Concepts and measures. *Catena* 24:215–232. doi:10.1016/0341-8162(95)00028-Q
- Ibáñez, J.J., R. Jiménez-Ballesta, and A. García-Álvarez. 1990. Soil landscapes and drainage basins in Mediterranean mountain areas. *Catena* 17:573–583. doi:10.1016/0341-8162(90)90031-8
- Ibáñez, J.J., A. Pérez, R. Jiménez-Ballesta, A. Saldaña, and J. Gallardo. 1994. Evolution of fluvial dissection landscapes in Mediterranean environments. Quantitative estimates and geomorphological, pedological and phytocenotic repercussions. *Z. Geomorph.* 38:105–119.
- Ibáñez, J.J., R. Pérez-Gómez, and F. San José Martínez. 2009. The spatial distribution of soils across Europe: A fractal approach. *Ecol. Complex.* 6:294–301. doi:10.1016/j.ecocom.2009.05.008
- Kim, J.W., E. Perfect, and H. Choi. 2007. Anomalous diffusion in two-dimensional Euclidean and prefractal geometrical models of heterogeneous porous media. *Water Resour. Res.* 43:W01405 doi:10.1029/2006WR004951.
- Luo, L., and H. Lin. 2009. Lacunarity and fractal analyses of soil macropores and preferential transport using micro-X-ray computed tomography. *Vadose Zone J.* 8:233–241. doi:10.2136/vzj2008.0010
- McBratney, A.B., I.O.A. Odeh, T.F.A. Bishop, M.S. Dumbar, and T.M. Shatar. 2000. An overview of pedometric techniques for use in soil survey. *Geoderma* 97:293–307. doi:10.1016/S0016-7061(00)00043-4
- Magurran, A.E. 1988. *Ecological diversity and its measurement*. Croom Helm, London. 179 pp.
- Mandelbrot, B. 1983. *The fractal geometry of nature*. W.H. Freeman and Co., New York.
- Myint, S.W., and N. Lam. 2005. A study of lacunarity-based texture analysis approaches to improve urban image classification. *Comput. Environ. Urban Syst.* 29:501–523. doi:10.1016/j.compenvurbsys.2005.01.007
- Pachepsky, Y.A., J.W. Crawford, and W.J. Rawls, editors. 2000. *Fractals in soil science*. Elsevier Sci., Amsterdam. 302 pp.
- Pendleton, D.E., A. Dathe, and P. Baveye. 2005. Influence of image resolution and evaluation algorithm on estimates of the lacunarity. *Phys. Rev. E* 72:041306. doi:10.1103/PhysRevE.72.041306.
- Phillips, J.D. 2001a. The relative importance of intrinsic and extrinsic factors in pedodiversity. *Ann. Assoc. Am. Geogr.* 91:609–621. doi:10.1111/0004-5608.00261
- Phillips, J.D. 2001b. Divergent evolution and spatial structure of soil landscape variability. *Catena* 43:101–113. doi:10.1016/S0341-8162(00)00122-3
- Plotnick, R.E., R.H. Gardner, W.W. Hargrove, K. Prestegard, and M. Perlmutter. 1996. Lacunarity analysis: A general technique for the analysis of spatial patterns. *Phys. Rev. E Stat. Phys. Plasmas Fluids Relat. Interdiscip. Topics* 53:5461–5468. doi:10.1103/PhysRevE.53.5461
- Plotnick, R.E., R.H. Gardner, and R.V. O'Neill. 1993. Lacunarity indexes as measures of landscape texture. *Landscape Ecol.* 8(3):201–211. doi:10.1007/BF00125351
- San José Martínez, F., and F.J. Caniego. 2013. Fractals and multifractals in pedodiversity and biodiversity analyses. In: J.J. Ibáñez and J. Bockheim, editors, *Pedodiversity*. Science Publ., Boca Raton, FL. p. 79–104.
- Turcotte, D.L. 1997. *Fractals and chaos in geology and geophysics*, 2nd ed. Cambridge Univ. Press, Cambridge, UK.
- Tyler, S.W., and S.W. Wheatcraft. 1989. Applications of fractal mathematics to soil water retention estimation. *Soil Sci. Soc. Am. J.* 53:987–996. doi:10.2136/sssaj1989.03615995005300040001x
- Zeng, Y., C.J. Gantzer, R.L. Payton, and S.H. Anderson. 1996. Fractal dimension and lacunarity of bulk density determined with X-ray computed tomography. *Soil Sci. Soc. Am. J.* 60:1718–1724. doi:10.2136/sssaj1996.03615995006000060016x